To Dr. Gkioulidou, Topical Editor

The submitted manuscript has been substantially revised by adding new sections 2 and 5 thereby increasing the number of pages from 13 to 18. Each issue has been addressed in the prescribed Comment/Response format. These responses were marked in the manuscript in bold and were specified by line numbers.

Point-by-point replies to the comments raised by Referee #1, a list of all relevant changes and marked-up manuscript are given below.

**Comment 1:**

"The author did not consider that magnetic field geometry changes during the expansion phase. As magnetic fluxes accumulate on closed field lines due to reconnection during the substorm expansion phase (together with earthward flows known as BBF), the magnetic field becomes more dipolar and the mapping location of a certain geocentric distance moves poleward. This geometrical change can easily explain the discrepancy between the poleward aurora motion and equatorward plasma drift. Please consider how mapping location changes by dipolarizing magnetic field will contribute to author's story."

Response:

Poleward expansion of auroras arising out of the onset arc was observed in the initial pulse of Pi2 pulsations [Saka et al., 2012]. Statistical study of geomagnetic fields at geosynchronous orbit during Pi2 showed that field line inclination at geosynchronous orbit (Goes5/6 at 285°/252° in geographic coordinates) decreased continuously in the growth phase and attained 33.6°/49.4° in dipole coordinates 2-min prior to the initial peak of Pi2 amplitudes (see Figure A below, reproduced from Saka et al., 2010). This result suggests the observed field line inclination prior to the onset conforms to T89 model of Kp=4 [Tsyganenko, 1989]. These field lines were mapped to auroral ionosphere at 63.4°N/62.7°N in geomagnetic coordinates corresponding to a latitude of onset arc. From these estimations, we suggest that Bursty Bulk Flows (BBFs) appeared first at the onset latitudes and activated preonset auroras. In the initial pulse of Pi2 pulsations, field line inclination of Goes5 increased in a step-like manner, while for Goes6 transient pulses were observed [Saka et al., 2010]. The average latitudes of Goes5 and Goes6 were at 10.3°N and 7.9°N, respectively in the T89 model for the average Kp index of 3. It is likely that dipolarization was composed of transient pulses at latitudes closer to the equatorial plane. In the following Pi2 pulses, an auroral surge was observed in

all-sky images between 66°N to 74°N in geomagnetic latitudes. They propagated eastward or westward at the poleward boundary of the auroral zone and were interpreted as an auroral manifestation of flow bifurcation of fast earthward flows (BBFs) [Saka et al., 2012].

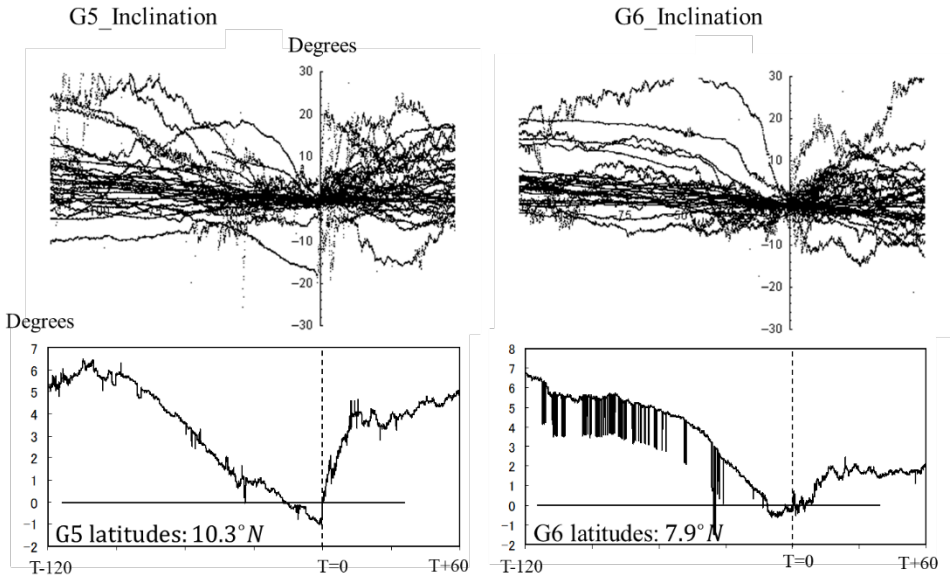


Figure A: Inclination angle in degrees measured positive northward from the V-D plane from 120 min prior to the Pi2 onset (T-120) and to 60 min after the Pi2 onset (T+60) reproduced from Saka et al. (2010). Magnetometer data of Goes 5/6 were represented in HVD coordinates, H is positive northward parallel to dipole axis, V is radial outward, and D is dipole east. Epoch superposition of 30 Pi2 events and mean angles calculated from them are plotted in top and in lower panels, respectively. Mean inclination angle at 2-min before the initial peak of Pi2 amplitudes was 33.6° for G5 and 49.4° for G6 in dipole coordinate. Dipolarization (T=0) was step-like at 10.3°N, while at 7.9°N it was composed of transient pulses.

Simultaneous with reconfigurations of field lines in meridional plane, field lines stretching initially in tailward directions switched to dawn-dusk directions in the initial pulse of Pi2s [Saka et al., 2000]. This switching was associated with the excitation of slow MHD wave by the increasing inflows of plasma sheet ions toward the equatorial plane in growth phase [Saka and Hayashi, 2017]. An alternative explanation for polarization switching may involve Ballooning instability of the coupled poloidal Alfven and slow magnetoacoustic modes [Rubtsov et al., 2018]. This switching from tailward to dawn-dusk directions disrupts the cross-tail currents creating a step like dipolarization or dipolarization pulses in the initial pulse of Pi2 pulsations and may produce convection surge and associated westward electric fields in the midnight sector.

Please refer to Lines 43 – 80 for more detail.

**Comment 2:**

"Equations (2) and (6) assume that there is no source term in the continuity equation. This assumption is not valid during the substorm expansion phase because of intense particle precipitation and vertical transport. Thus the density accumulation that the author obtained will be substantially modified. From this standpoint, the traffic flow analogy does not accurately represent the expansion phase. Please consider the effect of the source term."

Response:

For the equatorward drift in the flow channel to be an order of kilometers per second corresponding to E=100 mV/m in auroral ionosphere, both outflows and precipitation may not bring significant changes to the flux carried by $E \times B$ drift in the flow channel. We then approximate one dimensional (along the drift path) conservation equation in the flow channel.

Please refer to Lines 124 – 174, and 177 – 189 for more detail.

**Comment 3:**

"The author also assumes the one dimensional system. Expansion phase aurora including surges is two dimensional, where the electric field converges to the center of surges [Opgenoorth et al., 1983]. The distance between equipotential lines becomes larger when the electric field decreases. In this situation the density does not pile up but spreads azimuthally when the electric field decreases. The one dimensional assumption does not consider this effect."

Response:

We assume that the westward electric fields generated in the magnetosphere in the initial pulse of Pi2 pulsations were transmitted along the field lines to the auroral ionosphere by the guided poloidal mode [Radoski, 1967] from the surge location and created an equatorward flow in the auroral ionosphere. The flows are assumed to be confined in the flow channel expanding in the north-south directions in the midnight sector. The low-latitude end of the flow channel was at the latitudes of the onset arc corresponding to earthward edge of the BBFs. The high-latitude end may not expand beyond the poleward boundary of auroral zone. Longitudinal width of the flow channel may be in about 1 to 2 hours in local time (~1000 km along $65^{\circ}$N) corresponding to horizontal scale size of Pi2 vortices [Saka et al., 2014]. In this flow channel, two-dimensional potential structure grows.

In order to interrupt the excess accumulation in the flow channel, we suggested that ionosphere would have responded nonlinearly to decelerate the equatorward drifts in the flow channel. These were introduced by the ionospheric screening of the penetrated (total) electric fields. In this process, accumulated plasmas would have expanded backward while they were trapped in the flow channel.

Please refer to Lines 83 – 92 for more detail.

**Comment 4:**

"The author provided an equation for the shock front propagation but did not estimate if the speed is consistent with poleward expansion and if the critical density is within a realistic level of density in the ionosphere. Please make a quantitative assessment of this argument using realistic ionosphere parameters."

Response:

From the ionospheric screening process, we tentatively assume that flow velocity $U$ is a function of the density $n$. Then the conservation equation along the flow channel may be written as,

$$\frac{\partial n}{\partial t}+\frac{\partial}{\partial x}Q(n)=0\,. \qquad (9)$$

Here, $Q(n)$ is a mass flux defined by $Q(n)=nU(n)$. This relation can be reduced to nonlinear wave equation,

$$\frac{\partial n}{\partial t}+c(n)\frac{\partial n}{\partial x}=0\,. \qquad (10)$$

Here $c(n)$ is a wave propagation velocity defined by $c(n)=U(n)+nU'(n)$, $U(n)$ is a drift velocity in the flow channel, and $U'(n)$ denote braking/acceleration of the drift velocity by increasing and decreasing density. The equation (10) is often referred to as propagation of "kinematic waves" to describe traffic flow [Lighthill and Whitham, 1955]. In the following, we use dimensionless units normalized by $U_m$, and $n_m$. Here, $U_m$ and $n_m$ denote maximum drift velocity at $n$=0, and maximum density for the complete stops of the drift, respectively. Assuming a constant braking in the flow channel, we define $U$ by a linear function of density $n$ as $U(n)$=1-$n$. Noting that $Q'(n)=c(n)$, this relation is reduced to the equation, $Q(n)=n(1-n)$, identical to the case for the traffic flow [Whitham, 1999]. Both the $U$ *and* $Q$ are plotted in Figure 4A as a function of $n$. A nonlinear evolution of the waves is presented in Figure 4B by the characteristic curves. In the case of the traffic, the initial flows started from $n$=0 and stopped at $n$=1.0 by the tailback of cars. For the case of the ionosphere, the ionospheric density started from a finite density, $n$=0.3 (Figure 4B), and increased to $n$=1.0 to terminate the flow by the full screening. The nonlinear evolution of the density profile in time is shown in Figure 4B in colors from black ($T=T_1$), red ($T=T_2$), green ($T=T_3$), blue ($T=T_4$), and to purple ($T=T_5$). After $T=T_5$, the waves propagate upstream (poleward) as a shock. The shock velocity, $V$, is given as [Whitham, 1999],

$$V=\frac{Q(n_2)-Q(n_1)}{n_2-n_1}\,. \qquad (11)$$

Here, subscript 1 is for the values ahead shock and subscript 2 is for the values behind. Noting that

$Q(n_2)=0$ and substituting $Q(n_1)=n_1(n_2-n_1)$, the equation (11) can be reduced to $V=-n_1$ in dimensionless unit. The propagation velocity of the shock is related to the densities ahead. For the case of $n$=0.3 in Figure 4B, shock velocity can be estimated to be -0.3$U_m$. Here, $U_m$ denotes maximum drift velocity in the ionosphere where ionospheric screening effects vanished by the condition, $\Sigma_P/\Sigma_A << 1$.

Please refer to Lines 190 – 238 for more detail.

**Comment 5:**

"Figure 4 only provides the parallel velocity but what's important for poleward expansion is the poleward velocity."

Response:

We estimated parallel flow velocity generated by the transient accumulation in the flow channel. It may excite ion acoustic wave traveling upward from the peak of the F layer. A steady-state ion flows associated with the ion acoustic wave exist in the topside ionosphere and contribute to the vertical transport of materials from the ionosphere. This result was compared with the horizontal flows in the flow channel.

Please refer to Lines 124 -174.

Point-by-point replies to the comments raised by Referee #2, a list of all relevant changes and marked-up manuscript are given below.

**Comment 1:**

"In the current manuscript, a new scenario is proposed to explain how the ionospheric drift directions can be equatorward within the activated expansion-phase auroras while the poleward regions expand poleward. The main idea propose is that if one takes into account compressibility effect in the ionosphere, a sequence of events can potentially occur in which density accumulations in the ionosphere end up producing field aligned currents that propagate poleward. While the concept is interesting and is described in some detail, the manuscript does not present a self-consistent treatment in terms of real MI-coupling processes (no model really does this properly yet) and does not simulate any events that can be validated against observations. The simulations are fairly simplistic with questionable assumptions. For example, the evolution of density in equation (2) is treated as a 1D problem based on the assumption that the imposed convection surge spreads more widely in longitude than latitude. In addition, there in no model for how the "convection surge" is created or what might be going on in the tail that led to its creation. In real substorms, the magnetic field is highly variable including a slower stretching of the field during the growth phase followed by a more rapid and typically complex dipolarization phase. These B-field variations will change the mapping in a time dependent manner and produce a complex transient response in the form of MI-coupling which is not accounted for here. It is difficult to gauge how successful the model really is in terms of describing real substorms."

Response:

We added a new section with the title "Auroras and field line reconfigurations associated with Pi2" in Lines 43 - 80. This new section may respond to some extent to the comment above.

**Comment 2:**

"A major motivation of the manuscript appears to be the assumption that the direction of plasma drifts in the ionosphere during substorms is not understood. The author points out that the poleward expansion of the auroras [associated with substorms] is opposite to the general motion of plasma drift (or auroral forms?) within the expanding [bulge] (e.g. Lines 30-36 of the manuscript). As the author notes, this has been known for a very long time. Although it was not really discussed in the original phenomenological model of Akasofu et al. [1966]. That said, the author probably should not claim that this "discrepancy" has been source of ongoing debates since that time".

Response:

Sentences in the first version in Lines 30 – 36 were changed to:
"Plasma drifts in the ionosphere observed by the balloon-measured electric fields [Kelley et al., 1971], by the Ba releases [Haerendel, 1972] and by radar observations [Nielsen and Greenwald, 1978] did not match the expanding trajectories of auroras. This fact raises one of several unanswered questions involving violent poleward motion of auroras [Akasofu et al., 1966]. To account for the difference in propagation directions, it was suggested that auroras were directly connected to the reconnecting flux tube moving tailward in the plasma sheet. This idea suggests that the primary sources of particles are in the magnetosphere, though they might be accelerated in lower altitudes for precipitations. This concept has been accepted in the literature for many decades."
Please refer to Lines 23 -31.

**Comment 3:**
"Global aurora observations and ground-based all sky imagery clearly shows that while the envelop of activity expands poleward during the expansion phase, forms within the bulge tend to move equatorward. The Equatorward motion (often in the form of streamers) is completely consistent with the virtually universally-accepted idea that convection in the nightside magnetotail is Earthward (on the sunward side of reconnection sites) an that it is typically bursty in nature (i.e. bursty bulk flows described by Baumjohan, Angelopoulos, etc..). The poleward motion of the expanding envelop is also completely consistent with the progression of the substorm x-line toward the lobe field lines in the tail (and associated plasmoid release)."

Response:
Please refer our replies to Comment 6 for a response to the above comment.

**Comment 4:**
"The controversy addressed by THEMIS was not really about which direction auroral forms (or ionospheric plasma drifts) move during the expansion phase, but rather which region activates first (i.e. inside-out or outside-in) around a much narrower time period near the onset of a substorm. The controversies revolve around: (1) why in the outside-in model, auroral signatures of a higher latitude reconnection process are not clearly observed prior to the lower-latitude activation and subsequent poleward-expanding envelop, and (2) how in the inside-out model, a near-Earth disturbance is related to activation of mid-tail reconnection that is known to develop during substorms (and whose signatures have sometimes been reported to precede the lower latitude activation.)"

Response:
Please refer our replies to Comment 5 for a response to the above comment.

**Comment 5:**

"It appears to ignore mechanisms in the magnetotail that are already fairly well understood. For example, it is known that a new x-line is formed in the magnetotail sometime early on during substorms. In addition, it is known that convection from both the pre-existing x-line and the new substorm x-line proceeds in a bursty manner which produces Earthward-directed bursty bulk flows (BBFs). There has also been considerable work done in showing how such localized flows relate to equatorward-moving auroral forms in the ionosphere (i.e. streamers) and particle energization in the magnetosphere."

Response:

Poleward expansion of auroras arising out of the onset arc was observed in the initial pulse of Pi2 pulsations [Saka et al., 2012]. Statistical study of geomagnetic fields at geosynchronous orbit during Pi2 showed that field line inclination at geosynchronous orbit (Goes5/6 at $285^{\circ}/252^{\circ}$ in geographic coordinates) decreased continuously in the growth phase and attained $33.6^{\circ}/49.4^{\circ}$ in dipole coordinates 2-min prior to the initial peak of Pi2 amplitudes (see Figure A below, reproduced from Saka et al., 2010). This result suggests the observed field line inclination prior to the onset conforms to T89 model of Kp=4 [Tsyganenko, 1989]. These field lines were mapped to auroral ionosphere at $63.4^{\circ}$N/$62.7^{\circ}$N in geomagnetic coordinates corresponding to a latitude of onset arc. From these estimations, we suggest that Bursty Bulk Flows (BBFs) appeared first at the onset latitudes and activated preonset auroras. In the initial pulse of Pi2 pulsations, field line inclination of Goes5 increased in a step-like manner, while for Goes6 transient pulses were observed [Saka et al., 2010]. The average latitudes of Goes5 and Goes6 were at $10.3^{\circ}$N and $7.9^{\circ}$N, respectively in the T89 model for the average Kp index of 3. It is likely that dipolarization was composed of transient pulses at latitudes closer to the equatorial plane. In the following Pi2 pulses, an auroral surge was observed in all-sky images in $66^{\circ}$N to $74^{\circ}$N in geomagnetic latitudes. They propagated eastward or westward at the poleward boundary of the auroral zone and were interpreted as an auroral manifestation of flow bifurcation of fast earthward flows (BBFs) [Saka et al., 2012].

Please refer to Lines 43 – 80 in detail for new section titled "Auroras and field line reconfigurations associated with Pi2".

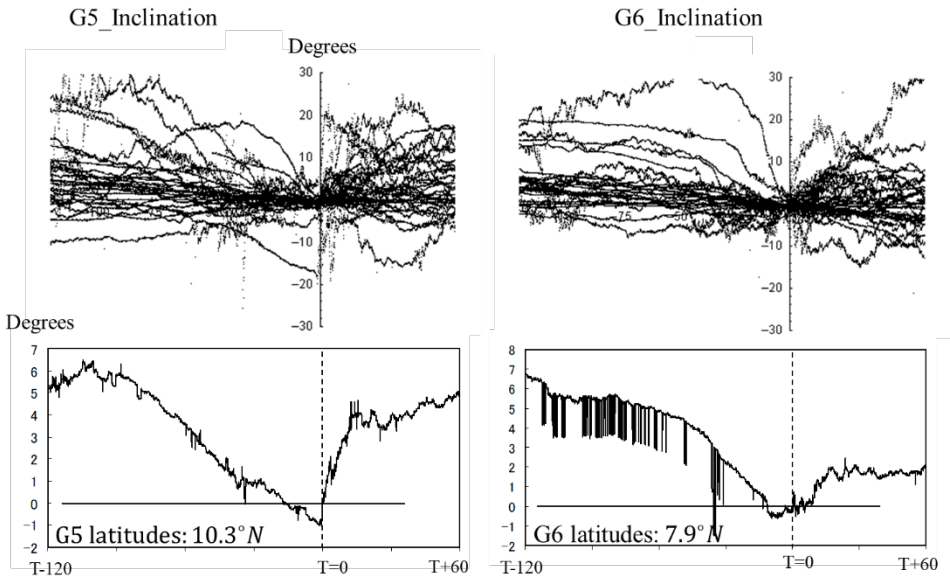


Figure A: Inclination angle in degrees measured positive from the V-D plane from 120 min prior to the Pi2 onset (T-120) and to 60 min after the Pi2 onset (T+60) reproduced from Saka et al. (2010). Magnetometer data of Goes 5/6 were represented in HVD coordinates, H is positive northward parallel to dipole axis, V is radial outward, and D is dipole east. Epoch superposition of 30 Pi2 events and mean angles calculated from them are plotted in top and in lower panels, respectively. Mean inclination angle at 2-min before the initial peak of Pi2 amplitudes was 33.6° for G5 and 49.4° for G6 in dipole coordinate. Dipolarization (T=0) was step-like at 10.3°N, while at 7.9°N it was composed of transient pulses.

**Comment 6:**

"Intensifications of the poleward expanding edge of the bulge are often accompanied by equatorward ejection of streamer form. How does the current model account for this type of activity? This is very easy to explain in the context of reconnection, but it is not clear how the current scenario would account for such observations."

Response:

Pi2 auroras were triggered by the onset of slow MHD wave excited by the inflows (Poynting flux) of plasma sheet ions towards the equatorial plane. In contrast, an evolution of N-S auroras (streamers) from the poleward auroral boundary occurred in association with a local enhancement of cross-tail electric fields but no inflows were observed that leads to the excitation of slow MHD wave [Saka et al., 2016]. These streamers may be observed in the intervals prior to the Pi2 onset [Nishimura et al., 2011]. In our scenario, streamers may not trigger the Pi2 onset.

Please refer to Lines 61 – 80 in detail.

References:

Saka, O., Hayashi, K., and Thomsen, M.F.: Equatorward evolution of auroras from the poleward auroral boundary, J.Atomos.Solar Terr.Phys., 145, 114-124, 2016.

Nishimura, Y., Lyons, L.R., Angelopoulos, V., Kikuchi, T., Zou, S., and Mende, S.B.: Relations between multiple auroral streamers, pre-onset thin arc formation, and substorm auroral onset, J.Geophys.Res., 116, doi:10.1029/2011JA016768, 2011.

**Comment 7:**

"Low-altitude observations have shown that the auroras at the poleward edge of the expanding disturbance are Alfvenic in nature (i.e. due to wave-accelerated electrons) (e.g. see Mende, (2016)). This is in contrast to more equatorward auroral arcs that are often associated with inverted-V type potential structures (acceleration of electrons through a field-aligned potential drop). It is not clear how the current model fits these observations. How does the model produce broadband wave acceleration of auroral particles at the poleward edge and inverted-V type structure in the more equatorward regions? The current scenario discusses ion acoustic wave travelling upward and downward along field lines in the ionosphere. Are these observed? How do they relate to observations of Alfvenic auroras already published?"

Response:

At the poleward boundary of auroral zone, fast aurora surge correlating to Pi2 pulse was observed in 66 – 74 ILat. Velocity of the surge, 12 - 30km/s at 100 km in altitudes, corresponds to azimuth flows of the order of 190 – 480 km/s at L=8.5 (70 ILat) [Saka et al., 2012]. It is supposed that these azimuthal flows may be an energy source exciting Alfven waves in the poleward boundary of auroral zone.

Parallel velocity that prevailed the ion acoustic phase velocity may excite a shock at the topside ionosphere (above 800 km for $T_e$=5000 K). The shock velocity may increase with altitudes in higher electron temperatures. A part of them would be observed as electrostatic shock or double layers at the altitudes of 6000 – 8000 km [Mozer et al., 1976; Temerin et al., 1982]. Those electrostatic shocks would have produced parallel potential structures referred to as inverted-V at the low latitude end of the flow channel. In this scenario, inverted-V as well as upward FACs are major components contributing to auroral acceleration in lower latitudes.

Ion acoustic waves related to auroral arcs were observed in the EISCAT radar echoes as naturally enhanced ion acoustic spectral shoulders [Wahlund et al., 1992]. The wavenumber spectrum of ion acoustic wave may not have a single peak at $10^{-6}$ $m^{-1}$ (1000 km) but spread to radar wavelength. In the present scenario, poleward boundary aurora surge is Alfvenic in nature and auroras in the flow channel

are of the inverted-V type.
Please refer to Lines 124 – 174 for more detail.

**Comment 8:**
"The poleward-expanding bulge during a substorm eventually grows to coalesce with the open-close boundary, while at the same time plasmoids are known to be released in the more distant tail. This is exceptionally strong evidence that new reconnection at a mid-tail site is a dominant driver during the expansion phase. It is not clear how the current model is consistent with these observations."

Response:
In nightside magnetosphere, Pi2 oscillations are regarded as a repeating flow bifurcation with a time constant of Pi2 periodicity (1-min), or flow diversion of BBF substructures [Saka et al., 2010]. If BBF substructures are related somewhat to the substorm cadence, Pi2 pulsations are geomagnetic manifestation of mid-tail reconnection repeated with the time constant of one minute.

**Comment 9:**
"The model assumes the imposition of physical processes and dynamics from the magnetotail in the form of a substorm "convection surge" at the dipolarization onset, but then argues that the ionosphere ends up directly driving processes in the tail (e.g. lines 199-202). It is probably more appropriate to think of the entire process via a more unified MI-coupling approach, but the fact that magnetotail processes appear to be required to drive the effects considered in the current model, indicates that the magnetosphere is really the source of driving in the model."

Response:
In the initial pulse of Pi2, flux tubes stretching in tailward directions switched to dawn-dusk directions through MHD processes. A possible candidate for the MHD processes is an excitation of slow MHD waves. This switching from tailward to dawn-dusk directions disrupts the cross-tail currents and produced convection surge and associated westward electric fields in the midnight sector. This MHD process (or instability) triggered the onset in the magnetosphere. In response to the onset, the ionosphere created parallel potential in the topside ionosphere which drove ion outflows, electron precipitations and upward field-aligned currents. A part of the upward field-aligned currents originated from the ionosphere may be observed at the geosynchronous orbit in the first 10 min intervals of Pi2 onset (see Figure B below).

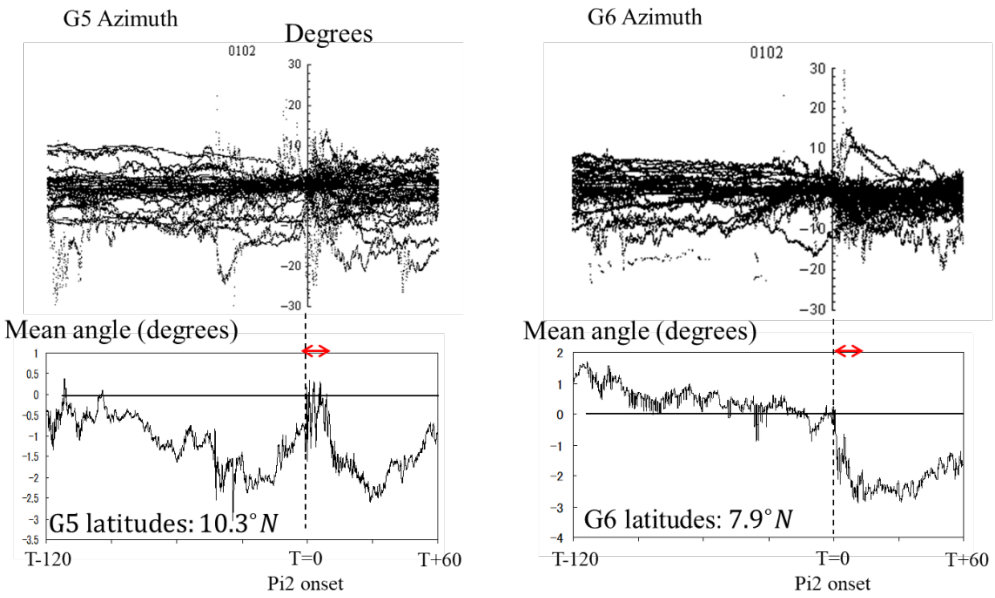


Figure B: Azimuth angle in degrees measured in the V-D plane positive counterclockwise from the V-axis from 120 min prior to the Pi2 onset (T-120) and to 60 min after the Pi2 onset (T+60) reproduced from Saka et al. (2010). Magnetometer data of Goes 5/6 were represented in HVD coordinates, H is positive northward parallel to dipole axis, V is radial outward, and D is dipole east. The azimuth angle is 180° when the field line vectors point earthward. Epoch superposition of 30 Pi2 events and mean angles calculated from them are plotted in top and in lower panels, respectively. Mean azimuth angle at 2-min before the initial peak of Pi2 amplitudes (T=0) was 183° for G5 and 180° for G6 in dipole coordinate. In the first 10 min intervals of Pi2 onset marked by red arrows, field line shears were observed between G6 and G5 latitudes. The shear is consistent with the field line change associated with the upward field-currents between the latitudes of G5 and G6 at 10.3°N and 7.9°N, respectively, in the T89 model for the average Kp index of 3.

Please refer to Lines 61 – 80 for more detail.

**Comment 10:**

"The manuscript should have described other models for poleward expansion of the aurora (as described in some of the points above), but one in particular has a very similar analogy to propagation of brake lights on cars in traffic. Specifically, the flow-braking model postulates a very similar tailward-propagating disturbance that could be related to poleward propagation in the ionosphere. Especially since the language used for these models is quite similar, the author should really have provided some discussion of it here".

Response:

We proposed the traffic flow analogy to explain the poleward expansion of auroras because of the

similarities in nonlinear processes in the flows. A similar case may be found in “flow braking in near-Earth tail” [Shiokawa et al., 1997].
Please refer to Lines 239 – 243.

**Comment 11:**

“In summary, the proposed model may be valuable in understanding some of the details of MI-coupling that occurs near onset, but it is very unlikely to be able to explain the full wealth of observations that are known to exist in the ionosphere and in the tail during expansion phase. In this view, the proposed scenario should not really be considered as an alternative to other models, but rather as a refinement on them. Otherwise, the author should be able to explain why all of the other mechanisms proposed in the past somehow cease to operate as a result of the currently proposed concept. For example, we know that near-Earth reconnection occurs during substorms. How does the current model stop this reconnection site from imposing a poleward-propagating envelop of activity in the ionosphere as it progresses toward the lobe field lines in the tail? Similarly, the manuscript does not address how the model is consistent with the vast array of known observations of aurora during substorms (e.g. how does it produce Alfvenic auroras at the poleward edge of the expanding bulge? How are streamer produced?)”

Response:

For our cases a new approach to auroral substorms developed from organizing the substorm processes in terms of the Pi2 pulsations observed in dip-equator; Huancayo in Peru and Christmas Island in Central Pacific. Low-latitude observations of geomagnetic Pi2 pulsations are believed to have some advantages in sorting out substorm cadence from the temporarily and spatially complexed processes in the magnetosphere.

# A new scenario applying traffic flow analogy to poleward expansion of auroras

Osuke Saka

Office Geophysik, Ogoori, Japan

**Abstract**

Transient westward electric fields from the magnetosphere generate equatorward plasma drifts of the order of kilometers per second in the auroral ionosphere. This flow channel extends in north-south directions and is produced in the initial pulse of Pi2 pulsations. Drifts in the ionosphere of the order of kilometers per second that accumulated plasmas at the low latitude end of the flow channel are of such large degree that possible vertical transport effects (including precipitation) along the field lines may be ignored. In order to interrupt the excess accumulation through the drift, we suggest that ionosphere responds nonlinearly to decelerate the equatorward drifts in the flow channel analogous to a traffic flow of cars on crowded roads. We apply this analogy to the poleward expansion of auroras.

## 1. Introduction

"Auroras and solar corona observed at the solar eclipse are optical phenomena unique in space physics. With enough knowledge about the underlying physical processes, once auroras have been captured by a highly sensitive imager, they provide an unexpected wealth of information about plasma environment of the Earth" [Oguti, 2010]. **Plasma drifts in the ionosphere observed by the balloon-measured electric fields [Kelley et al., 1971], by the Ba releases [Haerendel, 1972] and by radar observations [Nielsen and Greenwald, 1978] did not match the expanding trajectories of auroras. This fact raises one of several unanswered questions involving violent poleward motion of auroras [Akasofu et al., 1966]. To account for the difference in propagation directions, it was**

**suggested that auroras were directly connected to the reconnecting flux tube moving tailward in the plasma sheet. This idea suggests that the primary sources of particles are in the magnetosphere, though they might be accelerated in lower altitudes for precipitations. This concept has been accepted in the literature for many decades.**

It is worthy to consider whether the above idea also explains auroras associated with Pi2 pulsations. This is because Pi2 pulsations are accompanied by non-vortical slippage motions in the equatorial plane of midnight magnetosphere [Saka et al., 2007] while plasma motions in the auroral ionosphere were dominated by vortical flows [Saka et al., 2015]. The third harmonic deformations of the geomagnetic fields were generated in the midnight magnetosphere for tying two regions between slippage motions in the magnetosphere and vortical motions in the auroral ionosphere [Saka et al., 2012]. We may thus infer that vortical flows in the ionosphere do not originate in the magnetosphere but are rather generated in the ionosphere itself [Saka et al., 2012]. In this context, we interpret the motion of auroras as of ionospheric origin.

## 2. Auroras and field line reconfigurations associated with Pi2

**In Pi2 pulsations, poleward expansion of auroras arising out of the onset arc was observed in the initial pulse of Pi2 pulsations [Saka et al., 2012]. Statistical study of geomagnetic fields at geosynchronous orbit during Pi2 showed that field line inclination at geosynchronous orbit (Goes5/6 at 285°/252° in geographic coordinates) decreased continuously in the growth phase and attained 33.6°/49.4° in dipole coordinates 2-min prior to the initial peak of Pi2 amplitudes [Saka et al., 2010]. This result suggests the observed field line inclination prior to the onset conforms to T89 model of Kp=4 [Tsyganenko, 1989]. These field lines were mapped to auroral ionosphere at 63.4°N/62.7°N in geomagnetic coordinates corresponding to a latitude of onset arc. From these estimations, we suggest that Bursty Bulk Flows (BBFs) appeared first at the onset latitudes and activated preonset auroras. In the initial pulse of Pi2 pulsations, field line inclination of Goes5 increased in a step-like manner, while for Goes6 transient pulses were observed [Saka et al., 2010]. The average latitudes of Goes5 and Goes6 were at 10.3°N and 7.9**

°N, respectively in the T89 model for the average Kp index of 3. It is likely that dipolarization was composed of transient pulses at latitudes closer to the equatorial plane. In the following Pi2 pulses, an auroral surge was observed in all-sky images between 66°N to 74°N in geomagnetic latitudes. They propagated eastward or westward at the poleward boundary of the auroral zone and were interpreted as an auroral manifestation of flow bifurcation of fast earthward flows (BBFs) [Saka et al., 2012].

Simultaneous with reconfigurations of field lines in meridional plane, field lines stretching initially in tailward directions switched to dawn-dusk directions in the initial pulse of Pi2s [Saka et al., 2000]. This switching was associated with the excitation of slow MHD wave by the increasing inflows of plasma sheet ions toward the equatorial plane in growth phase [Saka and Hayashi, 2017]. After manipulating a set of linearized MHD equations [Kadomtsev, 1976], we have a relation between parallel shrinkage of plasmas along the field lines ( $\xi_z$ ) and perpendicular stretching of the field lines ( $\xi_\perp$ ) in the following form,

$$\xi_z = \frac{C_S^2}{\omega^2} F \cdot B_0^2 \frac{\partial}{\partial z}(div\xi_\perp) . \qquad (1)$$

Here, $C_s$, $\omega$ and $B_0$ are the sound velocity, angular frequency of waves and background field magnitudes, respectively. $F$ is given by $F = \frac{C_A^2}{B_0^2} \frac{1}{C_s^2 - (\frac{\omega}{k})^2}$ and is positive for the slow mode and negative for the fast mode. $C_A$ denotes Alfven velocity. If the wave mode was the fast mode, flux tubes would have contracted in longitudes towards the midnight sector, which was not observed during the first one-minute-interval of Pi2 onset (initial pulse of Pi2 onset). An alternative explanation of polarization switching may involve Ballooning instability of the coupled poloidal Alfven and slow magnetoacoustic modes [Rubtsov et al., 2018]. This switching from tailward to dawn-dusk directions disrupts the cross-tail currents creating a step like dipolarization or dipolarization pulses in the initial pulse of Pi2 pulsations and producing transient convection surge and associated westward electric fields in the midnight sector. The

**convection surge occurred once in the initial pulse of Pi2 pulsation but is not repeated in the following pulses.**

### 3. Horizontal plasma flows in the ionosphere

**It is reasonable to assume that westward electric fields were transmitted along the field lines to the auroral ionosphere by the guided poloidal mode [Radoski, 1967] from the surge location and created an equatorward flow through $E \times B$ drift of the order of kilometers per second in the auroral ionosphere. Electric fields of the order of 100 mV/m generate these high velocity flows in the ionosphere. The flows would be confined in a channel expanding in the north-south directions in the midnight sector. The low-latitude end of the flow channel was at the latitudes of the onset arc corresponding to earthward edge of the BBFs. The high-latitude end may not expand beyond the poleward boundary of auroral zone. Longitudinal width of the flow channel may be in about 1 to 2 hours of local time (~1000 km along 65°N) corresponding to horizontal scale size of Pi2 vortices [Saka et al., 2014].**

In the flow channel, drift across the magnetic fields for the *j-th* species ( $\mathbf{U}_{j\perp}$ ) can be written in the F region as [Kelley, 1989],

$$\mathbf{U}_{j\perp} = \frac{1}{B}[\mathbf{E} - \frac{k_B T_j}{q_j}\frac{\nabla n}{n}] \times \hat{\mathbf{B}}. \qquad (2)$$

Here, $\mathbf{E}$ denote westward electric fields in the flow channel and $\hat{\mathbf{B}}$ denotes a unit vector of the magnetic fields $B$, downward in the auroral ionosphere. Symbols $k_B$, $T_j$, $q_j$, and $n$ are the Boltzmann constant, temperature of the *j-th* species, charge of the *j-th* species, and density of electrons (ions), respectively. The electric field of the order of 100 mV/m exceeded the diffusion (second term) by three orders of magnitudes in low temperature ionosphere. The $E \times B$ drift predominated in the F region and diffusion term may be ignored. In the E region, drift trajectories may be written [Kelley, 1989] for electrons by,

$$\mathbf{U}_{e\perp} = \frac{1}{B}[\mathbf{E} \times \hat{\mathbf{B}}] \qquad (3)$$

and for ions by,

$$\mathbf{U}_{i\perp} = b_i[\mathbf{E} + \kappa_i \mathbf{E} \times \hat{\mathbf{B}}]. \qquad (4)$$

Here, $b_i$ is mobility of ions defined as $\Omega_i/(B\nu_{in})$, $\kappa_i$ is defined as $\Omega_i/\nu_{in}$. Symbols $\Omega_i$ and $\nu_{in}$ are ion gyrofrequency and ion-neutral collision frequency, respectively. $\hat{\mathbf{B}}$ denotes a unit vector of the magnetic fields $B$. To derive equations (3) and (4), pressure gradient term (diffusion) was again ignored. In the E region ($\kappa_i = 0.1$), although the first term of (4) exceeds the second term by one order of magnitudes, plasma accumulation in equatorward latitudes by the imposed westward electric fields was produced by equation (3) for electrons and the second term in (4) for ions. However, electron accumulation in lower latitudes increased southward electric fields and simultaneously ion drifts in the first term of (4). If the southward electric fields grew to exceed the westward electric fields by an order of magnitudes, ion drifts in the first term of (4) and electron drifts in (3) balanced to satisfy the quasi-neutrality. This is equivalent to the generation of the Pedersen currents in the ionosphere. Thus, electrostatic potential is generated in the E region, positive in poleward and negative in equatorward. The Pedersen currents would have closed to the field-aligned current (FAC) and sustain the steady state electrostatic potential produced in the ionosphere. Plasma drifts in the ionosphere, both in E and F regions, accumulate density at the low-latitude edge of the flow channel. In the following section, we discuss vertical transport of these accumulated materials from the low-latitude edge of the flow channel.

## 4. Vertical plasma flows in the ionosphere

**The transient compression of the ionospheric plasmas at the low-latitude edge of flow channel would excite the ion acoustic wave in the ionosphere travelling along the field lines upward and downward directions from the density peak of the F region. Figure 1 shows altitude distribution of the pre-onset density profile of electrons (black) and density profile caused by the accumulation in red. The accumulation doubled the electron density profile from 90 km to 1000 km in altitudes. Electron density profile in black was plotted using sunspot maximum condition**

130 **given in Prince and Bostic (1964). The travelling ion acoustic waves, upward and downward, are**
131 **denoted by vertical arrows. Ion acoustic wave propagating downward may be eventually**
132 **absorbed in the neutrals, while the upward wave may propagate along the field lines further**
133 **upward. We will focus only on the upward travelling ion acoustic wave. The ion acoustic wave**
134 **produced the parallel electric fields in accordance with the Boltzmann relation [Chen, 1974],**

135 $$E_{//} = -\frac{k_B T_e}{q}\frac{\nabla_{//} n_e}{n_e}. \qquad \textbf{(5)}$$

136 **Here,** $k_B$ **is Boltzmann constant,** $q$ **is electron charge,** $T_e$ **is electron temperature, and** $n_e$ **is**
137 **electron density (**$n_e = n_i$**). Equation (5) gives electric field strengths of the order of** $0.4\mu V/m$
138 **and** $2.0\mu V/m$ **for** $T_e = 1000K$ **and** $T_e = 5000K$**, respectively, when the e-folding distance**
139 **of density dropout along the filed lines was 200 km. For ions, steady-state motions exist in the**
140 **ionosphere in the altitudes where ion-neutral collision frequencies exceed ion acoustic wave**
141 **frequencies. In that case, parallel motions can be written as [Kelley, 1989],**

142 $$V_{i//} = b_i E_{//} - D_i \frac{\nabla_{//} n}{n} - \frac{g}{\nu_{in}}. \qquad \textbf{(6)}$$

143 **Here,** $b_i$ **and** $D_i$ **denote mobility and diffusion coefficient of ions defined by** $\frac{q_i}{M_i \nu_{in}}$ **and**
144 $\frac{k_B T_i}{M_i \nu_{in}}$ **, respectively. Symbols,** $M_i$**,** $q_i$**,** $\nu_{in}$**, and** $g$ **are ion mass, electric charge of ions,**
145 **ion-neutral collision frequency, and gravity, respectively. Ion-neutral collision frequencies from**
146 **400 km to 1000 km in altitudes were plotted in Figure 2 using nighttime sunspot maximum**
147 **condition in Prince and Bostick (1964). Frequencies of ion acoustic wave were calculated by**
148 **substituting wavelength of ion acoustic wave into the dispersion relation. The wavelength was**
149 **assumed to be identical to initial accumulation distance along the field lines. We chose two cases,**
150 **1000 km and 4000 km. Phase velocity of the ion acoustic wave of the order of 1600 m/s for the**
151 **electron temperatures of 5000K yields the wave frequencies of** $1.6\times10^{-3}s^{-1}$ **for the wavelength**
152 **of 1000 km and** $4.0\times10^{-4}s^{-1}$ **for 4000 km. These frequencies were overlaid in Figure 2.**

**Steady-state ion motions can be adopted up to 800 km, for a wavelength over 1000 km.**

**Altitude profile of steady-state ion flows were evaluated substituting 1000K for ion temperatures and the same e-folding distance in equation (5). Ions are oxygen and parallel electric fields are given by the equation (5). Snapshot of the velocity profile in altitudes from 400 km to 800 km is shown in Figure 3 for the two cases of electron temperatures, 5000K for black dots and 1000K for red dots. For the low temperature case (1000k), there occurred no ion upflow because the parallel electric fields could not overcome gravity. We suggest that electron temperatures over 2700K would be needed to excite ion upflow. When electron temperature was set to 5000K, ion velocity 15 m/s at 400 km in altitudes increased rapidly to 1369 m/s at 800 km. The altitude profile of the flow velocity in Figure 3 matched Type 2 ion outflow observed by EISCAT radar [Wahlund et al., 1992]. We conclude that the ion upflow in topside ionosphere was caused primarily by the parallel electric fields excited by the upward travelling ion acoustic wave. Below 600 km in altitudes, upflow velocity was one-to-two orders of magnitudes smaller than the equatorward drift in the flow channel. Upflow velocity became comparable to the horizontal drift over 800 km in altitudes and exceeded the phase velocity of ion acoustic wave. Parallel velocity that prevailed the ion acoustic phase velocity may excite a shock at the topside ionosphere. The shock velocity may increase with altitudes in higher electron temperatures. A part of them would be observed as electrostatic shock or double layers at the altitudes of 6000 – 8000 km [Mozer et al., 1976; Temerin et al., 1982]. Those electrostatic shocks would have produced parallel potential structures referred to as inverted-V at the low latitude end of the flow channel. In this scenario, inverted-V as well as upward FACs are major components contributing to auroral acceleration in lower latitudes.**

## 5. Nonlinear evolution of the horizontal flows

**Accumulation of electrons and ions occurred at the equatorward end of the flow channel. We can estimate a rate of accumulation by the following relation,**

$$\frac{\Delta n}{\Delta t} = -n_0 \frac{\Delta U}{\Delta x}. \qquad (7)$$

**Here *n* is plasma density, *U* denotes drift velocity in the flow channel in *x*. Substituting $\Delta U = 10^3 ms^{-1}$ and $\Delta x = 10^4 m$, we have $\frac{\Delta n}{\Delta t} = 10^{10} m^{-3} s^{-1}$ for the background density $n_0 = 10^{11} m^{-3}$. This gives density pileup of the order of $\frac{\Delta n}{n_0} = 100\%$ in ten seconds. If the equatorward drift in the flow channel is an order of $10^3$ m/s (E=100 mV/m in auroral ionosphere) and electron production by the precipitation do not exceed the accumulation rate which was 100% of the background density in ten seconds, both outflows and precipitation may not bring significant changes to the flux carried by $E \times B$ drift in the flow channel. We then approximate one dimensional (along the drift path in *x*) conservation equation in the flow channel.**

$$\frac{\partial n}{\partial t} + \frac{\partial}{\partial x}(nU) = 0 \qquad (8)$$

**A question arises regarding maximum accumulation of plasmas at the equatorward end of the flow channel because unlimited accumulation may not occur. One possible mechanism to suppress the accumulation may be associated with the ionospheric screening that decreased the amplitudes of penetrated (total) westward electric fields by the increasing ionospheric conductivities. In a two-dimensional ionosphere with uniform height-integrated conductivity, total electric fields *E* given by a sum of the incident ($E_i$) and reflected westward electric fields may be written as $E = \left(2\Sigma_A / \left(\Sigma_A + \Sigma_P\right)\right) E_i$, where $\Sigma_A$ and $\Sigma_P$ are Alfven conductance defined by $1/\mu_0 V_A$ and height-integrated Pedersen conductance in the ionosphere, respectively [Kan et al., 1982]. Symbols $\mu_0$ and $V_A$ denote magnetic permeability in vacuum and Alfven velocity, respectively. Amplitude ratio of total electric fields to incident electric fields is a function of conductance ratio of Pedersen and Alfven; $E/E_i = 2$ for a low conductivity of the ionosphere satisfying $\Sigma_P/\Sigma_A << 1$, and $E/E_i = 0$ for a high conductivity of the ionosphere satisfying**

$\Sigma_P/\Sigma_A >> 1$. **Noting that** $\Sigma_P$ **is proportional to the plasma density in the ionosphere, the total electric fields monotonically decreased with increasing plasma densities caused by accumulation itself and by the precipitations associated with the auroral activity. Another explanation may be suggested in the polarization electric fields (eastward) produced by the accumulation itself. These electric fields grew quickly with density accumulation and decreased the incident electric fields (westward) by the superposition. In addition to the above scenarios, we surmise that excess accumulation of the ionospheric plasmas may be suppressed through the term,** $(\mathbf{U}\cdot\nabla)\mathbf{U}$**, in the equation of motion. From the ionospheric screening process discussed above, we tentatively assume that flow velocity** ***U*** **is a function of the density** ***n*****. Then the conservation equation (8) may be written as,**

$$\frac{\partial n}{\partial t}+\frac{\partial}{\partial x}Q(n)=0\,. \qquad \textbf{(9)}$$

**Here,** ***Q(n)*** **is a mass flux defined by** ***Q(n)=nU(n)*****. This relation can be reduced to nonlinear wave equation,**

$$\frac{\partial n}{\partial t}+c(n)\frac{\partial n}{\partial x}=0\,. \qquad \textbf{(10)}$$

**Here** ***c(n)*** **is a wave propagation velocity defined by** $c(n)=U(n)+nU'(n)$**,** ***U(n)*** **is a drift velocity in the flow channel, and** ***U'(n)*** **denotes braking/acceleration of the drift velocity by increasing and decreasing density. The equation (10) is often referred to as propagation of "kinematic waves" to describe traffic flow [Lighthill and Whitham, 1955]. In the following, we use dimensionless units normalized by** $U_m$**, and** $n_m$**. Here,** $U_m$ **and** $n_m$ **denote maximum drift velocity at** ***n*****=0 and maximum density for complete stops of the drift, respectively. Assuming a constant braking in the flow channel, we define** ***U*** **by a linear function of density** ***n*** **as** ***U(n)*****=1-*****n*****. Noting that** ***Q'(n)=c(n)*****, this relation is reduced to the equation,** ***Q(n)=n(1-n)*****, identical to the case for the traffic flow [Whitham, 1999]. Both the** ***U and Q*** **are plotted in Figure 4A as a function of** ***n*****. A nonlinear evolution of the waves is presented in Figure 4B by the characteristic curves. In the case of vehicles in traffic, the initial flows started from** ***n*****=0 and stopped at** ***n*****=1.0 by the**

**tailback of cars. For the case of the ionosphere, the ionospheric density started from a finite density, $n$=0.3 (Figure 4B), and increased to $n$=1.0 to terminate the flow by the full screening. The nonlinear evolution of the density profile in time is shown in Figure 4B in colors from black ($T$=$T_1$), red ($T$=$T_2$), green ($T$=$T_3$), blue ($T$=$T_4$), and to purple ($T$=$T_5$). After $T$=$T_5$, the waves propagate upstream (poleward) as a shock. The shock velocity, $V$, is given as [Whitham, 1999],**

$$V = \frac{Q(n_2) - Q(n_1)}{n_2 - n_1}. \qquad \textbf{(11)}$$

**Here, subscript 1 is for the values ahead shock and subscript 2 is for the values behind. Noting that $Q(n_2)=0$ and substituting $Q(n_1)=n_1(n_2-n_1)$, the equation (11) can be reduced to $V = -n_1$ in dimensionless unit. The propagation velocity of the shock is related to the densities ahead. For the case of $n$=0.3 in Figure 4B, shock velocity can be estimated to be -0.3$U_m$. Here, $U_m$ denotes maximum drift velocity in the ionosphere where ionospheric screening effects vanished by the condition, $\Sigma_P / \Sigma_A << 1$.**

**We employed the traffic flow analogy to explain the poleward expansion of auroras. A similar case may be found in "flow braking in near-Earth tail" [Shiokawa et al., 1997]. In this case, the advective term in the equation of motion suppressed an excess pileup of the pressures caused by the fast earthward flow itself. This may minimize the velocity of the ion flows at the pressure peak analogous to a tailback of cars in traffic flows.**

## 6. Summary

Allowing for the compressibility of the ionosphere caused by the ionospheric drifts of the order of kilometers per second, we proposed a new scenario for the poleward expansion of auroras including generation of field-aligned currents and parallel electric fields of the ionospheric origin. This scenario, analogous to a traffic flow of cars on the crowded roads, partly explains the discrepant time history of the auroras which is often described as the auroras expand opposite to that of plasma drift in the ionosphere.

**Acknowledgements**

The author would like to express his sincere thanks to all the members of Global Aurora Dynamics Campaign (GADC) [Oguti et al., 1988]. We also gratefully acknowledge STEP Polar Network (http://step-p.dyndns.org/~khay/). Geomagnetic coordinates and footprints of the satellites are available at the Data Center for Aurora in NIPR (http://polaris.nipr.ac.jp/~aurora)

**References**

Akasofu, S.-I., Kimball, D.S., and Meng, C.-I.: Dynamics of the aurora-VII, Equatorward motions and the multiplicity of auroral arcs, J.Atmos.Terr.Phys., 28, 627-635, 1966.

Chen, F.F.: Introduction to plasma physics, Plenum Press, New York, 1974.

Haerendel, G.: Plasma drifts in the auroral ionosphere derived from Barium release, in Earth magnetospheric processes, B.M. McComac (ed), D.Reidel Publishing Company, 246-257, 1972.

Kadomtsev, B.B,: Collective phenomena in plasmas (in Japanese), Iwanami shoten, Tokyo, 1976.

Kan, J.R., Longenecker, D.U., and Olson, J.V.: A transient response of Pi2 pulsations, J.Geophys.Res., 87, 7483-7488, 1982.

Kelley, M.C., Starr, J.A., and Mozer, F.S.: Relationship between magnetospheric electric fields and the motion of auroral forms, J.Geophys.Res., 76, 5256-5277, 1971.

Kelley, M.C.: The earth's ionosphere: plasma physics and electrodynamics, Academic Press, Inc., 1989.

Lighthill, M.J., and Whitham, G.B.: On kinematic waves. II. A theory of traffic flow on long crowded roads, Proc. R. Soc. Lond. A, 229, 317-345, 1955.

Mozer, F.S., Carlson, C.W., Hudson, M.K., Torbert, R.B., Parady, B., Yatteau, J., and Kelley, M.C.: Observations of paired electrostatic shocks in the polar magnetosphere, Phys.Rew.Lett., 38, 292-295, 1977.

280 Nielsen, E., and Greenwald, R.A.: Variations in ionospheric currents and electric fields in association
281 with absorption spikes during substorm expansion phase, J.Geophys.Res., 83, 5645-5654,
282 1978.
283 Oguti, T., Kitamura, T., and Watanabe, T.: Global aurora dynamics campaign, 1985-1986,
284 J.Geomag.Geoelectr, 40, 485-504, 1988.
285 Oguti, T.: Introduction to auroral physics (in Japanese), Laboratory for Solar-Terrestrial Environment,
286 Nagoya University, 2010.
287 Prince, Jr., C.E., and Bostick, Jr., F.X.: Ionospheric transmission of transversely propagated plane
288 waves at micropulsation frequencies and theoretical power spectrums, 69, 3213-334, 1964.
289 Radoski, H.R.: Highly asymmetric MHD resonances: The guided poloidal mode, J.Geophys.Res., 72,
290 4026-4027, 1967.
291 Rubtsov, A., Mager, P.N., and Klimushkin, D.Yu.: Ballooning instability of azimuthally small scale
292 coupled Alfven and slow magnetoacoustic modes in two-dimensionally inhomogeneous
293 magnetospheric plasma, Phys.Plasmas, 25, doi:10.1063/1.5051474, 2018.
294 Runov, A., Angelopoulos, V., Zhou, X.-Z., Zhang, X.-J., Li, S., Plaschke, F., and Bonnell, J.: A
295 THEMIS multicase study of dipolarization fronts in the magnetotail plasma sheet,
296 J.Geophys.Res., 116, A05216, doi:10.1029/2010JA016316, 2011.
297 Saka, O., Akaki, H., Reeves, G.D., and Baker, D.N.: Magnetic fields and particle signatures in the
298 vicinity of nightside geosynchronous altitudes in the first one-minute-interval of Pi2 onset: a
299 case study, J.Atomos.Solar Terr.Phys., 62, 17-30, 2000.
300 Saka, O., Koga, D., and Hayashi, K.: A plasma bulk motion in the midnight magnetosphere during
301 auroral breakup inferred from all-sky image and magnetic field observations at
302 geosynchronous altitudes. J.Atomos.Solar Terr.Phys. 69, 1063-1074, 2007.
303 Saka, O. Hayashi, K, and Thomsen, M.: First 10 min intervals of Pi2 onset at geosynchronous altitudes
304 during the expansion of energetic ion regions in the nighttime sector, J.Atmos.Solar Terr.Phys.,
305 72, 1100-1109, 2010.

306 Saka, O., Hayashi, K., and Koga, D.: Periodic aurora surge propagating eastward/westward at
307 poleward boundary of aurora zone during the first 10 min intervals of Pi2 onset, J.Atmos.Sol.
308 Terr.Phys., 80, 285-295, doi:10.1016/j.jastp.2012.02.010, 2012.
309 Saka, O., Hayashi, K., and Koga, D.: Excitation of the third harmonic mode in meridian planes for Pi2
310 in the auroral zone, J.Geophys.Res., 117, doi:10.1029/2012JA018003, 2012.
311 Saka, O., Hayashi, K., and Thomsen, M.: Pre-onset auroral signatures and subsequent development of
312 substorm auroras: a development of ionospheric loop currents at the onset latitudes, Ann.
313 Geophys., 32, 1011-1023, 2014.
314 Saka, O., Hayashi, K., and Leonovich, A.S.: Explanation of Pi2 pulsations in auroral zone: Azimuthal
315 propagation of ionospheric loop currents, J.Geophys.Res., 120, doi:10.1002/2015JA021128,
316 2015.
317 Saka, O., and Hayashi, K.: Longitudinal expansion of field line dipolarization, J.Atomos.Solar
318 Terr.Phys., 164, 235-242, 2017.
319 Shiokawa, K., Baumjohann, W., and Haerendel, G.: Braking of high-speed flows in the near-Earth tail,
320 Geophys.Res.Lett, 24, 1179-1182, 1997.
321 Temerin, M., Cerny, K., Lotko, W., and Mozer, F.S.: Observations of double layere and solitary waves
322 in the auroral plasma, Phys.Rew.Lett., 48, 1176-1179, 1982.
323 Tsyganenko, N.A.: A magnetospheric magnetic field model with a warped tail current sheet. Planet.
324 Space Sci., 37, 5-20, 1989.
325 Wahlund, J.-E., Opgenoorth, H.J., Haggstrom, I., Winser, K.J., and Jones, G.O.: EISCAT observations
326 of topside ionospheric outflows during auroral activity: revisited, J.Geophys.Res., 97, 3019-
327 3017, 1992.
328 Whitham, G.B.: Linear and nonlinear waves, A Wiley-Interscience Publication, JOHN WILEY &
329 SONS, INC., 1999.
330
331
332

**Figure Captions**

**Fig. 1: Vertical profiles from 90 km to 1000 km in altitudes of electron number density in two conditions, pre-onset in black and after accumulation in red. Nighttime sunspot maximum condition given in Prince and Bostic (1964) was used to plot pre-onset condition. Vertical arrows directing upward and downward denote travelling ion acoustic waves propagating along the field lines from the density peak of F layer.**

**Fig.2: Ion-neutral collision frequency ( $\nu_{in}$ ) in altitudes from 400 km to 1000 km calculated using nighttime sunspot maximum condition in Prince and Bostick (1964). Wave frequencies of ion acoustic wave are overlaid for two wavelength, 1000 km and 4000 km along field lines (see text).**

**Fig. 3: Steady-state parallel velocity in altitudes for ions (oxygen) produced by parallel electric fields $0.4\mu V/m$ ($T_e$=1000K) in red dots and $2.0\mu V/m$ ($T_e$=5000K) in black dots. Vertical flows in altitudes from 400 km to 800 km are shown. Flow velocity is positive upward and negative downward.**

**Fig. 4: (A) Normalized flux($Q$)-density($n$) curve (thin curve) and velocity(U)-density(n) line (thick line) in flow channel. Vertical scale of $U$-$n$ line is shown to the right, scale of $Q$-$n$ curve is to the left. Dotted line at $n$=0.5 indicates the critical density where $c(n)$ vanishes; waves are stationary relative to the ground. Waves propagate forward/backward at a density below/above the critical density. (B) Nonlinear evolution of the density accumulation. Density increased in a step like manner from $T_1$ to $T_5$. Shock velocity is 1.2 km/sec poleward when $U_m$=4.0 km/s is assumed at $n$=0.3 (see text).**

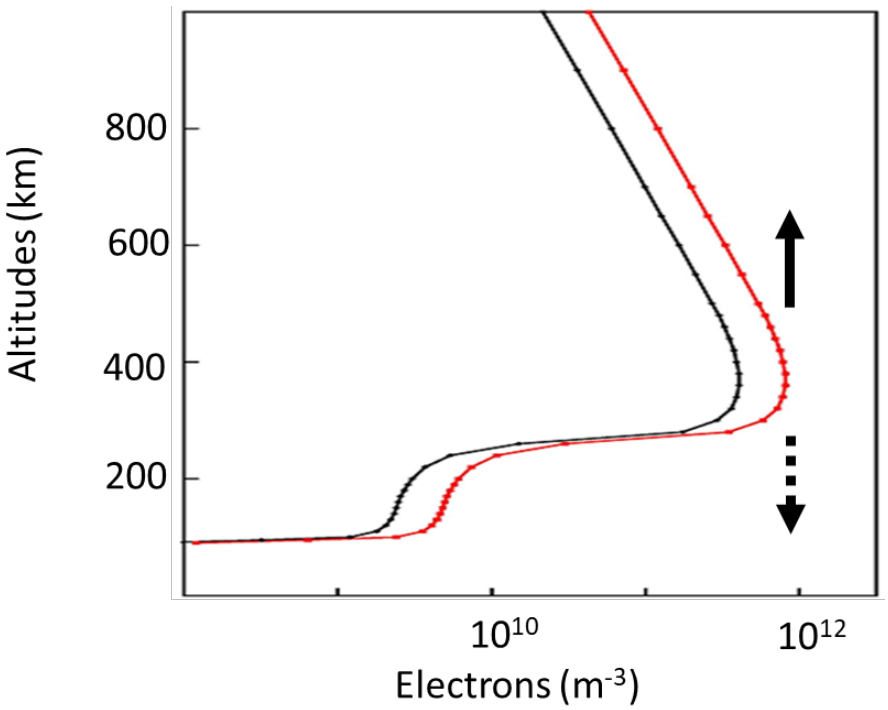


Figure 1

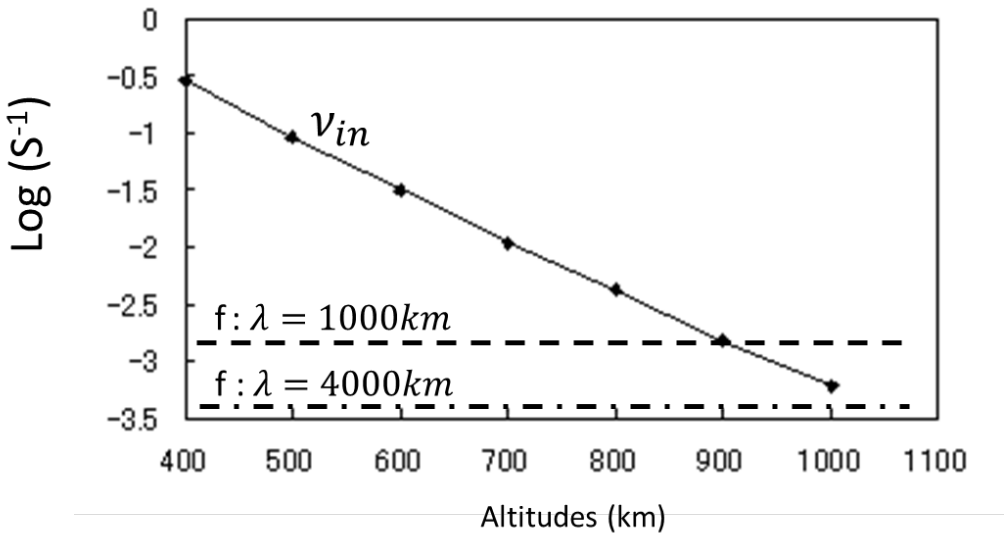
0
-0.5
-1
-1.5
-2
-2.5
-3
-3.5
Log ($S^{-1}$)
$\nu_{in}$
f : $\lambda = 1000km$
f : $\lambda = 4000km$
400
500
600
700
800
900
1000
1100
Altitudes (km)

Figure 2

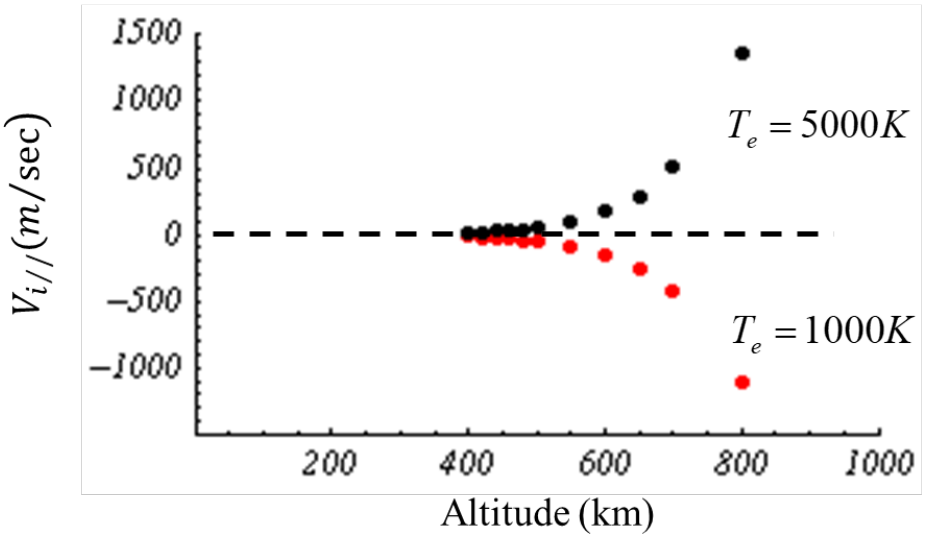
1500
1000
500
0
−500
−1000
$V_{i//}(m/\sec)$
$T_e = 5000K$
$T_e = 1000K$
200
400
600
800
1000
Altitude (km)

Figure 3

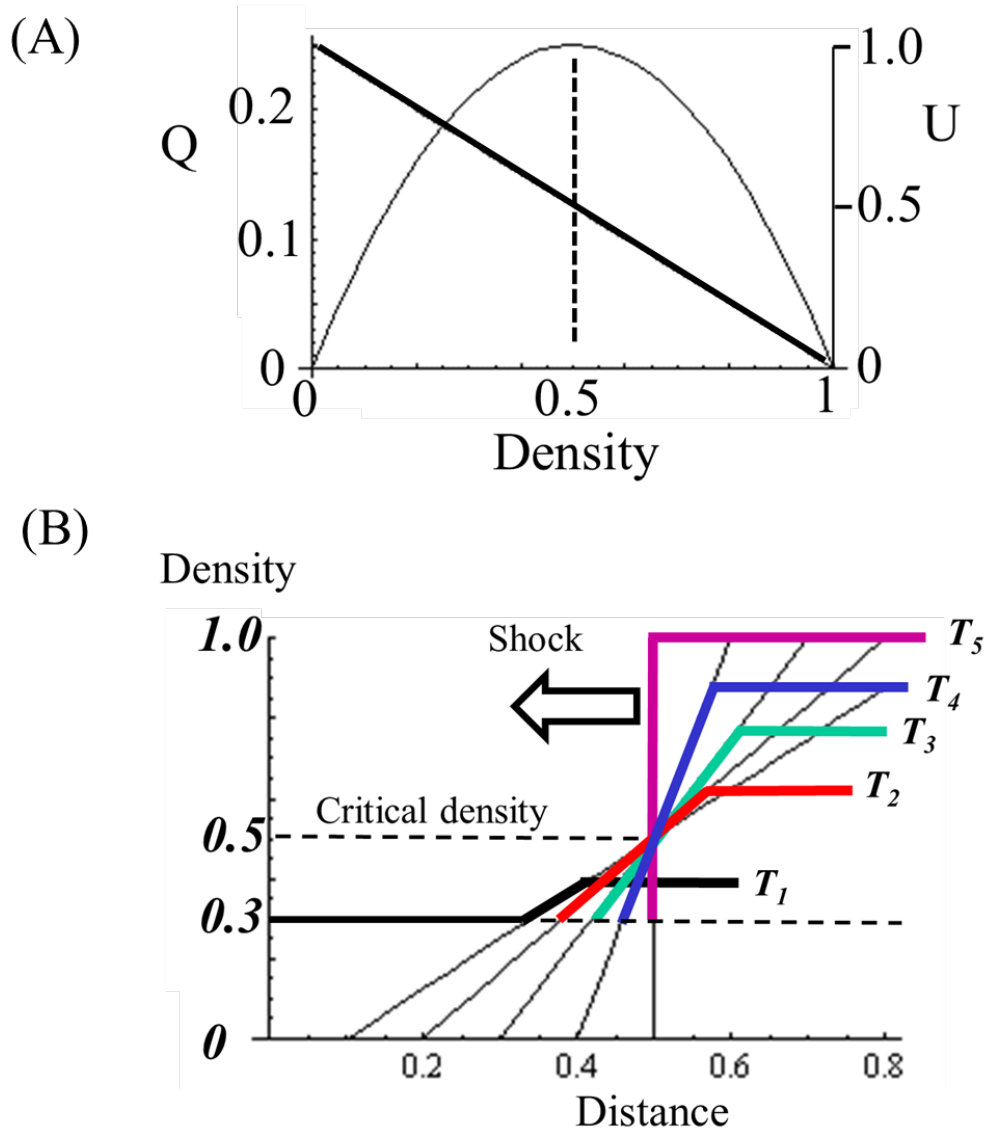
(A)
Q
0.2
0.1
0
1.0
U
0.5
0
0
0.5
1
Density
(B)
Density
1.0
0.5
0.3
0
Shock
Critical density
$T_5$
$T_4$
$T_3$
$T_2$
$T_1$
0.2
0.4
0.6
0.8
Distance

Figure 4